1-1-2007

Design and analysis of transmission-level power system stability control

Tu Phan
Ryerson University

DESIGN AND ANALYSIS OF TRANSMISSION-LEVEL POWER SYSTEM STABILITY CONTROL

by

Tu Phan

Bachelor of Engineering, Toronto, 1997

A project
presented to Ryerson University
in partial fulfillement of the
requierments for the degree of
Master of Engineering
in the Program of
Electrical & Computer Engineering

Toronto, Ontario, Canada, 2007

AUTHOR'S DECLARATION

I hereby declare that I am the sole author of this project.

I authorize Ryerson University to lend this project to other institutions or individuals for the purpose of scholarly research.

Signature:_____

I further authorize Ryerson University to reproduce this project by photocopying or by other means, in total or in part, at the request of other institutions or individuals for the purpose of scholarly research.

Signature:_____

INSTRUCTIONS ON BORROWERS

Ryerson University requires the signatures of all persons using or photocopying this project. Please sign below, and give address and date.

Name	Signature	Address	Date

ACKNOWLEDGMENTS

The author wishes to express sincere appreciation to my supervisor Dr. Richard Cheung, for his input in the preparation of this project report. I sincerely appreciate the valuable advices, professional guidance, and consistent encouragement from Dr. Richard Cheung throughout all stages of my study.

I would like to thank Dr. Fei Yuan and Dr. Mehmet Zeytinoglu for their continuous encouragement during my graduate study.

TABLE OF CONTENTS

LIST OF FIGURES

Chapter 1

INTRODUCTION

1.1 Motivation

A successful operation of a power system is to provide reliable and uninterrupted power to the loads. Ideally, the loads should be fed by the utility supply at constant voltage and frequency at all times. In practical terms, this means that both the voltage and frequency of the utility supply must be held at the nominal values within a small tolerance, so that the consumer's equipment can operate properly. For example, a drop in voltage of 10-15% may lead to stalling of the motor loads on the system.

A requirement of reliable electricity supply is to ensure that generators have adequate capacity to meet the load demands. If at any time a generator loses synchronism with the rest of the system, substantial voltage and current fluctuations may occur and as a result, transmission lines may be automatically tripped by their relays and the tripping may occur at critical locations. If a generator is separated from the system due to loss of synchronism, the generator has to be resynchronized in order to continuous supplying the power system, assuming it has not been damaged and its prime mover has not been shut down due to the disturbance. The loss of synchronism in generators is a serious power system stability problem [1-2].

Power interruptions in the high-voltage transmission system connecting the generating stations and the load centers are virtually unavoidable, particularly due to natural causes such as lightning and ice storm. Such interruptions are often the causes of the power system stability problems that can affect considerably the

power flow to a large geographical area and as a result, this can cause tremendous economical loss.

Because of its important economical impact, the power system stability has continuously received a great deal of attention, due to the fact that the electrical power system is often subjected to various disturbances. The stable operation of the power system generator and its ability to maintain the quality electrical powers delivered to the consumers at the minimum generation cost with maximum possible power transfer are the key requirements in the design of an electrical power system. The effective and popular approach of achieving the stable operation for the generator is to provide an efficient controller for the generator excitation system.

The design of a power system stabilizer (PSS) is based on the idea that the use of a supplementary control signal in the excitation system of the generating unit can provide extra damping for the system and resulting in high dynamic performance of the generator. This is an effective, economic and flexible way to improve power system stability. Over the past few decades, many types of PSS controllers such as the optimal control, adaptive control, fuzzy logic control, and etc., have been extensively studied and some of them have been successfully used in the field [3].

The main focus of study in this paper is on an investigation into the conventional power system stabilizer (PSS) controller design, methods of combining the PSS with the automatic voltage regulator (AVR) excitation controller. The operation of PSS controller for enhancement of the stability of the power system, particularly after the power system has been affected by disturbances such as a three-phase fault occurring near the generator bus, is presented followed by Matlab/Simulink simulations. Furthermore, emphasis will be given to the

transient behavior of the system which is described mathematically by ordinary differential equations.

1.2 Objective

The objective of this project is to design and analyze an optimal control of the generator excitation based on the model of lead-lag power system stabilizer. The project also focuses on power system stability, particularly after the power system is subjected to severe disturbances, such as a three-phase fault, occurring on or near the generator bus.

1.3 Outline

Chapter 1: introduces the problem of stability in the power system.

Chapter 2: presents a brief review of the cause of power system oscillation, the need for generator excitation control. A combination of the classical automatic voltage regulator and power system stabilizer is also discussed in this section. In addition, the chapter presents the modeling of synchronous generator, power system network, excitation system for the design of an optimal excitation control in this project.

Chapter 3: presents Matlab/Simulink computer simulations of the lead-lag power system stabilizer design.

Chapter 4: Highlights the conclusions of the work in the project and suggests future work in this area.

Chapter 2

POWER SYSTEM MODEL

In this section, the study provides a summary of the causes of power system oscillations, the need for generator excitation control, the combination of the automatic voltage regulator and power system stabilizer.

In order to assess the stability of power system, adequate mathematical models describing the system are needed. The models must be computationally efficient and be able to represent the power system.

A realistic power system is seldom at steady-state. Such a state never exists in the true sense [4]. Random changes in load are taking place at all times, with subsequent adjustments of generation. Furthermore, major changes do take place at times, e.g., a fault on the network, failure in a piece of equipment, sudden application of a major load such as a steel mill, or loss of a line or generating unit. The disturbances could be a large disturbance such as tripping of generator unit, sudden major load change and fault switching of transmission line etc. The system behavior following such a disturbance is critically dependent upon the magnitude, nature and the location of fault and to a certain extent on the system operating conditions. The stability analysis of the system under such conditions, normally termed as "Transient-stability analysis", is generally attempted using mathematical models involving a set of non-linear differential equations.

In contrast to this disturbance-specific transient instability, there exists another class of instability called the "dynamic instability" or more precisely "small oscillation instability". As the small oscillation stability is concerned with small

excursions of the system about a quiescent operating point, the system can be sometimes approximated by a "linearized model" about the particular operating point. Once a valid linearized model is available, the powerful and well established techniques of linear control theory can be applied for stability analysis and performance evaluation of various power system stabilizers.

Nonlinear models on the other hand have more realistic representation of the power systems. Designing controllers for such nonlinear systems is more difficult. In this study, a non-linear model of single generator infinite bus system has been considered for the excitation control design and performance analysis. The generator model is mechanical power input invariant. Furthermore, the model is expressed in *dq0* reference frame, which rotates with the rotor, for the simplification of design and evaluation.

2.1 Brief summary of power system generator excitation control

The control of generator excitation is needed for maintaining the power system stability. The basic function of an excitation system is to provide a direct current to the synchronous generator field winding. Excitation controls functions of both adjusting voltage and damping oscillation by controlling the field voltage.

The stability problem is concerned with the behavior of the synchronous machines after they have been perturbed. If the perturbation does not involve any net change in power, the machines should return to their original state.

When a disturbance such as a three phase fault occurs at or near the generator bus, the output terminal of the power system generator will be affected immediately. The flow of electrical power to the power system network is interrupted during the fault, and the generator rotor speed is advanced by the input mechanical power. As the fault happened in the network, the protection circuit has activated to clear the fault. After the fault, the generator attempts to

reconnect to the power system network to restore the electrical power supply. During the recovery process, the generator is often subjected to some form of post fault oscillations. This is caused by the energy stored in the advancement of generator rotor during the period of fault. Damper windings on the generator rotor can be used to control the oscillation but this technique is not cost effective. A more effective method in terms of cost and control is the generator excitation control.

A traditional generation excitation control is the automatic voltage regulator (AVR) that regulates the generator terminal voltage based on the terminal voltage feedback. Basically, in order to restore the terminal voltage to its pre-fault value, the AVR increases the level of the field voltage. The recovery of terminal voltage is fast for the AVR control. However, there is a negative effect on the damping of post fault oscillation because the oscillating torque, which causes system oscillations, increases relatively to the terminal voltage.

The combination of a power system stabilizer (PSS) and AVR excitation controller could help to eliminate negative damping effects due to post fault oscillation. However, the combination of PSS and AVR controllers need to be designed properly, or the generator under control may lose synchronism in an attempt to control its excitation field [5].

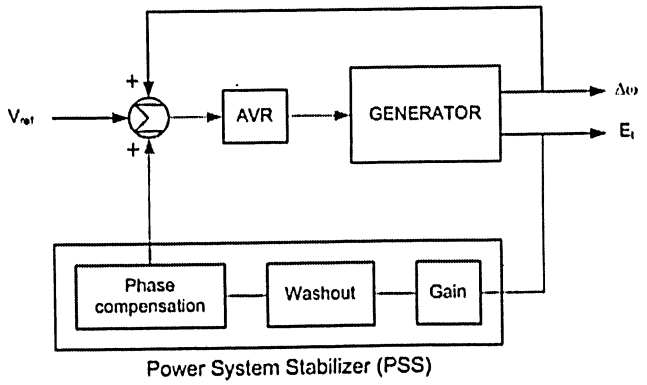

Figure 2.1: Block diagram of the AVR and PSS excitation control

The block diagram of AVR and PSS excitation control is shown in Figure 2.1. Some control signals are used for the PSS such as the rotor speed deviation ($\Delta\omega$), the electric power (ΔP), or the generator frequency (Δf). These signals are feedback signals which used to produce a damping torque control component. Since the main action of the PSS is to control the rotor oscillations, the most frequently used control signal for the PSS is the speed signal.

The output signal of any PSS controller is a voltage signal. The particular PSS structure contain a washout block, which is used to limit the over response of the damping during severe events. Since the PSS must produce a component of electrical torque in phase with the speed deviation, the phase-lead block circuits are used to compensate for the lag between the PSS output and the control action, the electrical torque.

All of the variables of the PSS must be determined for each type of generator separately because of the dependence on the machine parameters. The power system dynamics also affect the PSS values. In this paper, the power system stabilizer is designed based on the model of a single machine connected to an infinite bus system (SMIBS) under given operating condition.

The AVR and PSS excitation control technique is the popular choice in practice for damping rotor oscillations. However, the AVR/PSS controller associates with some drawbacks [1,6]. The AVR and PSS are usually designed independently from each other. The former is designed to satisfy the required voltage regulation performance, and the later is designed to damp the rotor oscillations. Since the designed objectives for the two controllers are different, it can be difficult to archive a totally satisfactory design for damping oscillations when the operation conditions change.

Another drawback is that the PSS are tuned around a steady-state operating point. Since the PSS only operate in a narrow band of oscillating frequencies, its damping effect is only valid for small excursions around this operating point. In fact, during severe disturbances, a PSS may actually cause the generator to lose its synchronism.

An automatic voltage regulator (AVR), coupled with a power system stabilizer (PSS), play a fundamental role in the dynamical behavior of power systems. In fact, for damping oscillations, an automatic voltage regulator (AVR) is not sufficient, and using power system stabilizers (PSS) is necessary. Therefore, a good generator terminal voltage controller should combine an AVR with a PSS. The AVR and PSS design should have a good robustness against significant changes in the characteristics of the network. It has been shown that for a combination of an AVR with a PSS to be robust, both of them should be coordinated, i.e., they should not be designed in an independent manner.

2.2 Generator model

There are several models which have been used in modeling synchronous machines for stability studies, some including damper windings and transient flux linkages, some neglecting them.

The stator of a typical synchronous generator holds a three-phase winding where the individual phase windings are distributed 120° apart in space. The rotor holds a field winding together with one or two damper windings, which are magnetized by a DC field current. This section presents the generator model in both the balanced three-phase stationary '*abc*' and the synchronously rotating '*dq0*' variables.

Synchronous machine model in the balanced three-phase 'abc' variables

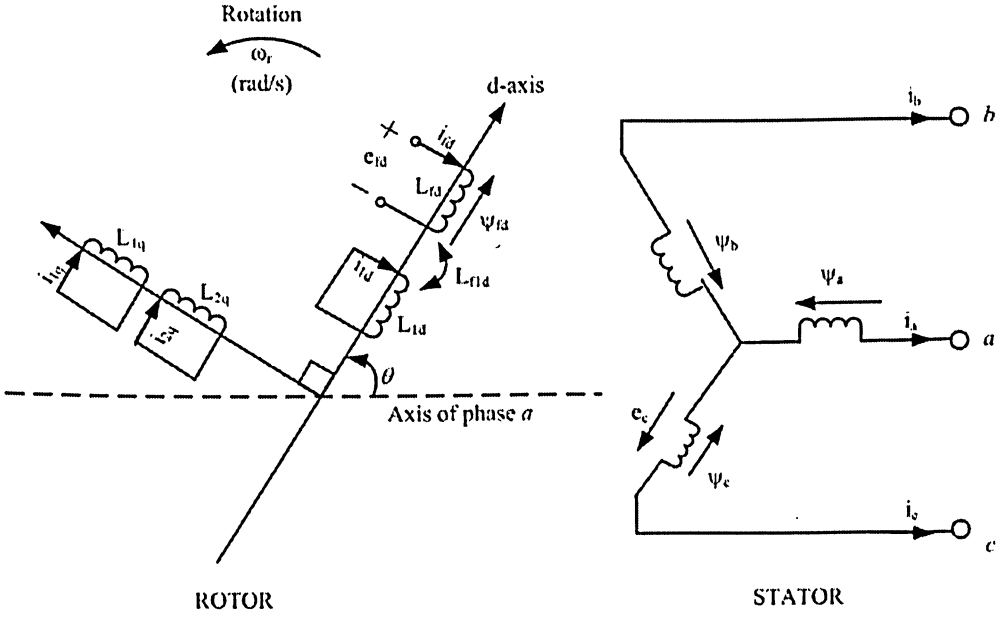

Figure 2.2: Stator and rotor circuits of synchronous generator model

Figure 2.2 shows a simplified circuit model for a typical synchronous machine. The magnetic axis of the field winding is called as the rotor direct axis (d-axis). The rotor quadrature axis (q-axis) is perpendicular to the field winding magnetic d-axis.

From the diagram, the generator stator has three symmetrical windings in stationary '*abc*' axes at 120° apart. The rotor includes field and damper windings in the d-axis and two other damper windings in the q-axis. The generator flux and current relationship can be determined as,

$$\begin{pmatrix} \psi_{abcs} \\ \psi_{dqr} \end{pmatrix} = \begin{pmatrix} L_s & L_{sr} \\ L_{sr}^T & L_r \end{pmatrix} \cdot \begin{pmatrix} -i_{abcs} \\ i_{dqr} \end{pmatrix} \tag{2.1}$$

where,

$\psi_{abcs} = \begin{pmatrix} \psi_a & \psi_b & \psi_c \end{pmatrix}^T$: represent the three-phase stator winding flux linkage

$\psi_{dqr} = \begin{pmatrix} \psi_{fd} & \psi_{1d} & \psi_{1q} & \psi_{2q} \end{pmatrix}^T$: represent the rotor winding flux linkage

$i_{abs} = \begin{pmatrix} i_a & i_b & i_c \end{pmatrix}^T$: represent the three-phase stator winding current

$i_{dqr} = \begin{pmatrix} i_{fd} & i_{1d} & i_{1q} & i_{2q} \end{pmatrix}^T$: represent rotor winding current

The stator winding inductance matrix is defined as

$$L_s = \begin{bmatrix} L_{aa} & L_{ab} & L_{ac} \\ L_{ba} & L_{bb} & L_{bc} \\ L_{ca} & L_{cb} & L_{cc} \end{bmatrix}$$

where,

$L_{aa} = L_{aa0} + L_{aa2}\cos 2\theta$ represents phase *a* self-inductance

$L_{bb} = L_{aa0} + L_{aa2}\cos 2(\theta - 2\pi/3)$ represents phase *b* self-inductance

$L_{cc} = L_{aa0} + L_{aa2}\cos 2(\theta + 2\pi/3)$ represents phase *c* self-inductance

$L_{ab} = L_{ba} = -L_{ab0} - L_{ab2}\cos(2\theta + \pi/3)$ represents phase *a* to phase *b* mutual inductance

$L_{ac} = L_{ca} = -L_{ab0} - L_{ab2}\cos(2\theta - \pi/3)$ represents phase *a* to phase *c* mutual inductance

$L_{bc} = L_{cb} = -L_{ab0} - L_{ab2}\cos(2\theta - \pi)$ represents phase *b* to phase c mutual inductance

In Figure 2.2, θ is defined as the angle by which the d-axis leads the centre line of phase *a* winding in the direction of rotation. Since the rotor is rotating with

respect to the stator, angle θ is related to the rotor angular velocity ω_r and time t as follows,

$$\theta = \omega_r t$$

The rotor winding inductance matrix is defined as

$$L_r = \begin{bmatrix} L_{ffd} & L_{f1d} & 0 & 0 \\ L_{f1d} & L_{11d} & 0 & 0 \\ 0 & 0 & L_{11q} & L_{12q} \\ 0 & 0 & L_{12q} & L_{22q} \end{bmatrix}$$

where,

L_{ffd}: self-inductance of the field winding

L_{11d}, L_{11q}, L_{22q}: self-inductances of the dq-axis damper windings respectively

L_{f1d}: mutual-inductance between the field and damper windings in the d-axis

L_{12q}: mutual-inductance between the two damper windings in the q-axis

The generator stator and rotor mutual inductances are determined by,

$$L_{sr} = \begin{bmatrix} L_{afd}\cos\theta & L_{a1d}\cos\theta & -L_{a1q}sin\theta & -L_{a2q}\sin\theta \\ L_{afd}\cos(\theta - 2\pi/3) & L_{a1d}\cos(\theta - 2\pi/3) & -L_{a1q}\sin(\theta - 2\pi/3) & -L_{a2q}\sin(\theta - 2\pi/3) \\ L_{afd}\cos(\theta + 2\pi/3) & L_{a1d}\cos(\theta + 2\pi/3) & -L_{a1q}\sin(\theta + 2\pi/3) & -L_{a2q}\sin(\theta + 2\pi/3) \end{bmatrix}$$

where,

L_{afd}, L_{a1d}, L_{a1q}, L_{a2q}: the peak mutual inductances between the stator and rotor windings

The generator terminal voltages can be determined by,

$$\begin{bmatrix} e_{abs} \\ e_{dqr} \end{bmatrix} = \begin{bmatrix} R_s & 0 \\ 0 & R_s \end{bmatrix} \begin{bmatrix} -i_{abcs} \\ i_{dqr} \end{bmatrix} + p \begin{bmatrix} \psi_{abcs} \\ \psi_{dqr} \end{bmatrix} \qquad (2.2)$$

where,

$e_{abs} = \begin{bmatrix} e_a & e_b & e_c \end{bmatrix}^T$: three-phase stator winding voltage

$e_{dqr} = \begin{bmatrix} e_{fd} & 0 & 0 & 0 \end{bmatrix}^T$: rotor winding voltage with the short-circuited damper windings

$R_s = diag\begin{bmatrix} R_a & R_a & R_a \end{bmatrix}$: three-phase stator winding resistance matrix

$R_r = diag\begin{bmatrix} R_{fd} & R_{1d} & R_{1q} & R_{2q} \end{bmatrix}$: winding resistance matrix

The above Equations (2.1) and (2.2) are the mathematical model for a synchronous machine in the balanced three-phase '*abc*' variables. This model is not convenient for the mathematical computation. The reason is that the stator winding inductances L_s and the mutual inductances L_{sr} between the stator and field windings are dependent on the rotor position angle θ, which in turn, varies with time.

The '*dq0*' transformation

The '*dq0*' transformation is introduced to simplify the mathematical computation as shown in Equations (2.1). Basically, the stator voltage and current variables are established by appropriate transformation, which is known as Park's transformation.

Assume that the 'dq' axes are oriented at θ angle, and $x_a + x_b + x_c = 0$. The transformation of the three-phase abc variables to the equivalent two-phase dq variables can be determined as

$$\begin{bmatrix} x_d \\ x_q \\ x_0 \end{bmatrix} = \frac{2}{3}\begin{bmatrix} \cos\theta & \cos(\theta - 2\pi/3) & \cos(\theta - 4\pi/3) \\ -\sin\theta & -\sin(\theta - 2\pi/3) & -\sin(\theta - 4\pi/3) \\ 1/2 & 1/2 & 1/2 \end{bmatrix} \cdot \begin{bmatrix} x_a \\ x_b \\ x_c \end{bmatrix}$$

where x_a, x_b and x_c can represent current, voltage or flux linkage.

Similarly, the corresponding inverse relation *dq* to *abc* is

$$\begin{bmatrix} x_a \\ x_b \\ x_c \end{bmatrix} = \begin{bmatrix} \cos\theta & -\sin\theta & 1 \\ \cos(\theta - 2\pi/3) & -\sin(\theta - 2\pi/3) & 1 \\ \cos(\theta - 4\pi/3) & -\sin(\theta - 4\pi/3) & 1 \end{bmatrix} \cdot \begin{bmatrix} x_d \\ x_q \\ x_0 \end{bmatrix}$$

If the transformation matrix is named as P, the stator and rotor flux-current linkage relationship from Equation (2.1) can be expressed in dq0 components as follows,

$$\begin{bmatrix} \psi_{dq0s} \\ \psi_{dqr} \end{bmatrix} = \begin{bmatrix} PL_s P^{-1} & PL_{sr} \\ L_{sr}^T P^{-1} & L_r \end{bmatrix} \begin{bmatrix} i_{dq0s} \\ i_{dqr} \end{bmatrix} \tag{2.3}$$

where,

$$PL_{sr} = \frac{3}{2} \begin{bmatrix} L_{afd} & L_{a1d} & 0 & 0 \\ 0 & 0 & -L_{a1q} & -L_{a2q} \\ 0 & 0 & 0 & 0 \end{bmatrix}$$

$$L_{sr}^T P^{-1} = \frac{3}{2} \begin{bmatrix} L_{afd} & 0 & 0 \\ L_{a1d} & 0 & 0 \\ 0 & -L_{a1d} & 0 \\ 0 & -L_{a2q} & 0 \end{bmatrix}$$

$$PL_s P^{-1} = diag\begin{bmatrix} L_d & L_q & L_0 \end{bmatrix}$$

and,

$$\begin{cases} L_d = L_{aa0} + L_{ab0} + \frac{3}{2} L_{aa2} \\ L_q = L_{aa0} + L_{ab0} - \frac{3}{2} L_{aa2} \\ L_0 = L_{aa0} - 2L_{ab0} \end{cases} \qquad \begin{cases} L_d = L_l + L_{ad} \\ L_q = L_d + L_{aq} \end{cases}$$

The above variables are defined as follows,

L_d, L_q : the *dq*-axis inductance

L_0: the zero sequence inductance

L_l: the leakage inductance

L_{ad}, L_{aq}: the mutual inductances associated with the air-gap leakage flux linkages due to the currents i_d and i_q, respectively

As shown in Equation (2.3), the varying rotor angle θ, which affected the generator stator and rotor inductances, has been eliminated after applying the dq0 transformation into Equation (2.1). Hence, the analysis of the synchronous machine model is now less complicated.

From Equation (2.2), the stator voltage equations in *dq0* components are as follows,

$$\begin{aligned} e_{dq0s} &= -i_{dq0s}R_s + Pp(P^{-1}\psi_{dq0s}) \\ &= -i_{dq0s}R_s + PP^{-1}p\psi_{dq0s} + P(pP^{-1})\psi_{dq0s} \\ &= -i_{dq0s}R_s + p\psi_{dq0s} + \omega_r\begin{bmatrix}\psi_q & \psi_d & 0\end{bmatrix}^T \end{aligned} \tag{2.4}$$

where,

$$\omega_r = \frac{d\theta}{dt} = 2\pi f \quad \text{electrical (rad/s)}$$

and

p: denotes for the time derivative.

The generator voltage equation matrix representation is as follows,

$$\begin{bmatrix} e_d \\ e_d \\ e_d \\ e_d \\ 0 \\ 0 \\ 0 \end{bmatrix} = \begin{bmatrix} R_a & 0 & 0 & 0 & 0 & 0 & 0 \\ 0 & R_a & 0 & 0 & 0 & 0 & 0 \\ 0 & 0 & R_a & 0 & 0 & 0 & 0 \\ 0 & 0 & 0 & R_{fd} & 0 & 0 & 0 \\ 0 & 0 & 0 & 0 & R_{1d} & 0 & 0 \\ 0 & 0 & 0 & 0 & 0 & R_{1q} & 0 \\ 0 & 0 & 0 & 0 & 0 & 0 & R_{2q} \end{bmatrix} \begin{bmatrix} -i_d \\ -i_q \\ -i_0 \\ i_{fd} \\ i_{1d} \\ i_{1q} \\ i_{2q} \end{bmatrix} + p \begin{bmatrix} \psi_d \\ \psi_q \\ \psi_0 \\ \psi_{fd} \\ \psi_{1d} \\ \psi_{1q} \\ \psi_{2q} \end{bmatrix} + \omega_r \begin{bmatrix} -\psi_q \\ \psi_d \\ 0 \\ 0 \\ 0 \\ 0 \\ 0 \end{bmatrix} \quad (2.5)$$

The zero-sequence component in Equation (2.3) and (2.5) can be eliminated if the system is balanced. In addition, the term of $p\psi_{dq0s}$ can also be negligible because it is small and decays fast in post disturbance analysis. The Equation (2.5) can be expressed in a simplified form,

$$\begin{cases} e_d = -R_a i_d - \omega_r \psi_q \\ e_q = -R_a i_q + \omega_r \psi_d \end{cases} \quad (2.6)$$

The generator three-phase terminal electrical power is determined as follows,

$$\begin{cases} P_t = e_a i_a + e_b i_b + e_c i_c \\ P_t = e_d i_d + e_q i_q \end{cases} \quad (2.7)$$

The electromagnetic power P_e is a combination of the terminal power and the losses on the stator winding resistance. By substituting (2.6) into (2.7), the P_e can be written as below,

$$\begin{aligned} P_e &= P_t + (i_d^2 + i_q^2) R_a \\ &= \omega_r (\psi_d i_q - \psi_q i_d) \end{aligned} \quad (2.8)$$

Again, ω_r is defined as the generator rotor speed in electrical radians per second.

Using (2.8), the electric torque can be expresses as follows,

$$T_e = \frac{P_e}{\omega_{mech}}$$
$$= \frac{\omega_r(\psi_d i_q - \psi_q i_d)}{\omega_{mech}}$$
$$= \frac{n_p}{2}(\psi_d i_q - \psi_q i_d) \qquad (2.9)$$

where,
ω_{mech}: represents the rotor speed in mechanical radians per second
n_p: represents the number of poles

Per unit generator excitation control system representation

A per unit system is used to normalize power system variables. Compared with employing physical units in system equations, such as amperes, volts, ohms, henrys, etc., the per unit normalization can eliminate units and express system quantities as dimensionless ratios. As a result, the design analysis and computational efforts are simpler and more convenient. In general, the quantity in per unit is written as,

$$\text{quantity in per unit} = \frac{\text{actual quantity}}{\text{base value of quantity}}$$

Considering a power system generator model which is expressed in the per unit system, the simplifications of its variables and equations are listed as follows,

The mutual inductances between the stator and rotor windings with respect to the stator and rotor sides at each axis:

$$\overline{L}_{ad} = \overline{L}_{afd} = \overline{L}_{a1d} \tag{2.10}$$

The generator torque:

$$\overline{T}_e = \overline{\psi}_d \overline{i}_q - \overline{\psi}_q \overline{i}_d \tag{2.11}$$

The stator voltage equations:

$$\begin{aligned} \overline{e}_d &= -\overline{R}_a \overline{i}_d - \overline{\psi}_q \\ \overline{e}_q &= -\overline{R}_a \overline{i}_q + \overline{\psi}_d \end{aligned} \tag{2.12}$$

Note that the generator speed ω_r is equal to 1 after the per unit normalization in the above stator voltage equations.

The above generator terminal voltage, stator flux and current, from the equation matrix (2.5), can be re-written in the per unit system as follows,

$$\begin{cases} e_d = -\psi_q - R_a i_d \\ e_q = \psi_d - R_a i_q \end{cases} \tag{2.13}$$

Also, the change of the generator rotor flux, damping current and excitation voltage in dq reference frame:

$$\begin{cases} p\psi_{fd} = \omega_0 (e_{fd} - R_{fd} i_{fd}) \\ p\psi_{1d} = -\omega_0 R_{1d} i_{1d}) \\ p\psi_{1q} = -\omega_0 R_{1q} i_{1q}) \\ p\psi_{2q} = -\omega_0 R_{2q} i_{2q}) \end{cases} \tag{2.14}$$

Note that, the bar notation for a per-unit quantity is omitted in the above equations for simplification.

The derivation of mathematical equations of (2.13) and (2.14) are used to serve the following purposes:

- Connecting the generator model to the power system network model for simulations of various power system disturbances
- Providing a mathematical relationship for generator excitation control
- Studying of the oscillation damping effects on the generator control

The generator rotor motion equation is expressed as follows,

$$\begin{cases} p\Delta\omega_r = (T_m - T_e - K_D\Delta\omega_r)/2H \\ p\delta = \omega_0\Delta\omega_r \end{cases} \tag{2.15}$$

where,
$T_e = \psi_d i_q - \psi_q i_d$: the generator electrical torque in pu
$\Delta\omega_r$: the change of rotor angular velocity
δ : the rotor angular position
H : the moment of inertia in second
K_D : the damping factor

The above equation (2.15) represents the mechanical characteristics of a synchronous machine as well as the difference between the electromagnetic and mechanical torques.

2.3 The generator *dq*-axis model

While the above Equations (2.12) to (2.14) can be used to analyze a synchronous generator's performance, it is a common practice to use equivalent circuits to provide a visual description of the machine model.

In this section, the standard generator model with the three damper windings and the simplified generator model without any damper winding are discussed. While the later model is used for simplifying the design of the generator control, the former one is commonly used in simulations for better results and accuracies.

The sixth-order generator model with damper windings

The general equivalent circuits which represent the complete characteristics, including the synchronous machine voltage equations, are shown in Figure 2.3. The voltages and flux linkage are present in the circuits. Note that the flux linkages are shown in terms of their time derivatives.

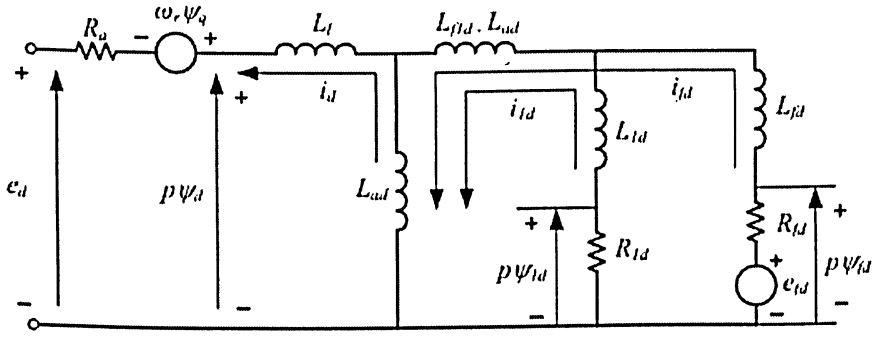

(a) d-axis equivalent circuit

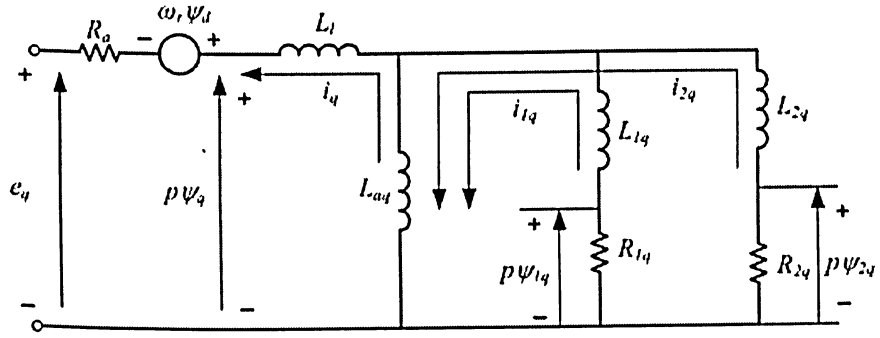

(b) q-axis equivalent circuit

Figure 2.3: Complete d- and q-axis equivalent circuits

The d-axis air-gap flux linkage is used to determine the mutual inductance between the damper winding at d-axis and field winding L_{f1d}. This result is approximately equal to L_{ad}. Similarly, the mutual inductance between the two damper windings at q-axis L_{12q} is close to L_{aq}. Therefore, it is widely assumed that $L_{f1d} = L_{ad}$ and $L_{12q} = L_{aq}$ in the power system stability study.

The other self-inductances L_{ffd}, L_{11d}, L_{11q} and L_{22q} are combinations of the leakage inductance and mutual inductances as follows,

$$\begin{cases} L_{f1d} = L_{ad} \\ L_{12q} = L_{aq} \\ L_{ffd} = L_{fd} + L_{ad} \\ L_{11d} = L_{1d} + L_{ad} \\ L_{11q} = L_{1q} + L_{ad} \\ L_{22q} = L_{2q} + L_{ad} \end{cases} \tag{2.16}$$

The flux linkages of the synchronous generator can be written in the matrix form by using the equations from (2.16) as below,

$$\begin{bmatrix} \psi_d \\ \psi_q \\ \psi_{fd} \\ \psi_{1d} \\ \psi_{1q} \\ \psi_{2q} \end{bmatrix} = \begin{bmatrix} L_d & 0 & L_{ad} & L_{ad} & 0 & 0 \\ 0 & L_d & 0 & 0 & L_{aq} & L_{aq} \\ L_{ad} & 0 & L_{ffd} & L_{ad} & 0 & 0 \\ L_{ad} & 0 & L_{ad} & L_{11d} & 0 & 0 \\ 0 & L_{aq} & 0 & 0 & L_{11q} & L_{aq} \\ 0 & L_{aq} & 0 & 0 & L_{aq} & L_{22q} \end{bmatrix} \begin{bmatrix} -i_d \\ -i_q \\ i_{fd} \\ i_{1d} \\ i_{1q} \\ i_{2q} \end{bmatrix} \tag{2.17}$$

Figure 2.4 is shows the simplified equivalent circuits of the synchronous generator with three damper windings in the *dq0* reference frame. The equivalent circuits are based on the Equations (2.13), (2.14) and (2.17), which express the

relationship between flux linkages and currents. This circuit model is popular and widely accepted in power utility applications.

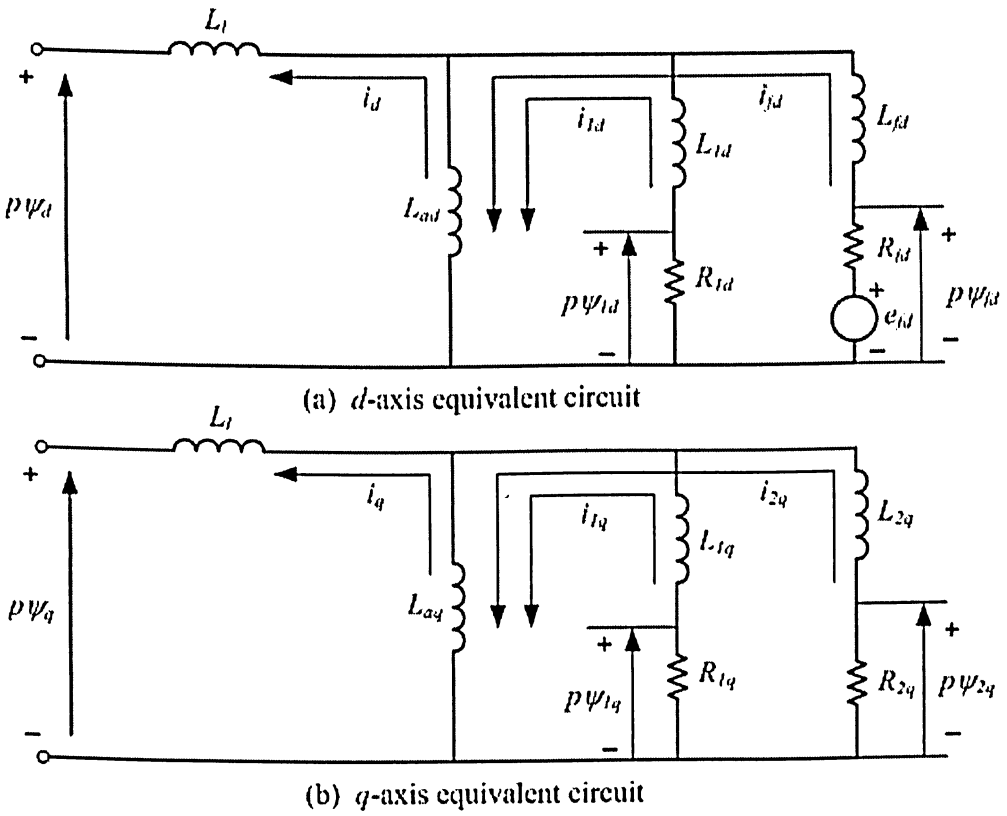

Figure 2.4: Commonly used simplified d- and q-axis equivalent circuits of a synchronous generator with three damper winding

As shown in Figure 2.4, the d-axis flux linkage ψ_d is a combination of the leakage flux linkage, which produced by the current i_d through L_l, and the air-gap flux linkage ψ_{ad} produced by the current i_d through L_{ad}. Similarly, the q-axis flux linkage ψ_q is a combination of the leakage flux linkage, which produced by the current i_q through L_l, and the air-gap flux linkage ψ_{aq} produced by the current i_q through L_{aq}.

The d- and q-axis equivalent circuits also do not present the stator resistance, voltage drops, and the speed voltage terms.

From Equations (2.13), (2.14) and (2.17), the voltage, current and flux linkage relationships are summarized as follows,

$$\begin{cases} p\psi_{fd} = \omega_0 (e_{fd} - R_{fd} i_{fd}) \\ p\psi_{1d} = -\omega_0 R_{1d} i_{1d} \\ p\psi_{1q} = -\omega_0 R_{1q} i_{1q} \\ p\psi_{2q} = -\omega_0 R_{2q} i_{2q} \\ p\Delta\omega_r = (T_m - T_e - K_D \Delta\omega_r)/2H \\ p\delta = \omega_0 \Delta\omega_r \end{cases} \quad \begin{cases} e_d = -\psi_q - R_a i_d \\ e_q = \psi_d - R_a i_q \\ \psi_d = \psi_{ad} - i_d L_l \\ \psi_q = \psi_{aq} - i_q L_l \\ i_{fd} = (\psi_{fd} - \psi_{ad})/L_{fd} \\ i_{1d} = (\psi_{1d} - \psi_{ad})/L_{1d} \\ i_{1q} = (\psi_{1q} - \psi_{aq})/L_{1q} \\ i_{2q} = (\psi_{2q} - \psi_{aq})/L_{2q} \end{cases} \tag{2.18}$$

As shown in Equation (2.18), all the machine quantities are in the per-unit system, while the time and angles are in seconds and radians respectively. The synchronous machine model is called the 6th-order generator model because it consists of six coupled differential equations. This model will be employed in the project for the study of the generator excitation control and simulations.

The third-order generator model without damper windings

The *dq0*-axis equivalent circuit of a synchronous generator without dampers is shown in Figure 2.5 and is a simplification of the 6th-order model.

The machine equations of (2.18) can be simplified as follows,

$$\begin{cases} p\psi_{fd} = \omega_0 (e_{fd} - R_{fd} i_{fd}) \\ p\Delta\omega_r = (T_m - T_e - K_D \Delta\omega_r) / 2H \\ p\delta = \omega_0 \Delta\omega_r \end{cases} \qquad \begin{cases} e_d = -\psi_q - R_a i_d \\ e_q = \psi_d - R_a i_q \\ \psi_d = \psi_{ad} - i_d L_l \\ \psi_q = \psi_{aq} - i_q L_l \\ i_{fd} = (\psi_{fd} - \psi_{ad}) / L_{fd} \end{cases} \tag{2.19}$$

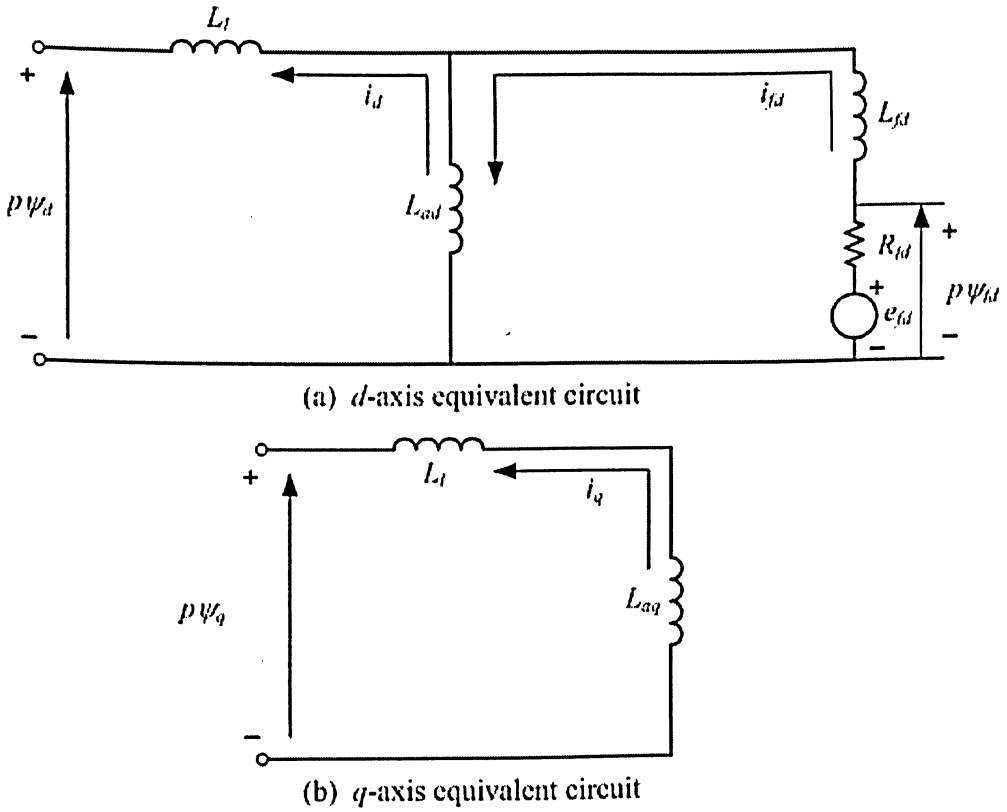

Figure 2.5: d- and q- axis equivalent circuits of a synchronous generator without damper winding

Since the damper windings are omitted from the circuits, the equations' order is reduced. Therefore, the computations and design analysis are less complex due to the lower order model. However, the model does introduce some errors.

2.4 Transmission network model

Figure 2.6 show a typical single machine to infinite bus system model for testing and evaluation of the generator excitation control design. The simplified power transmission network model is a Thevenin equivalent circuit. The equivalent circuit consists of an equivalent network transmission line impedance $Z_L = R_L + jX_L$ and an infinite bus voltage source, V_B.

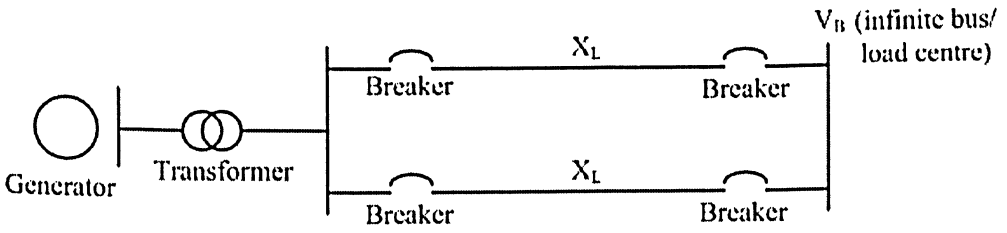

Figure 2.6a: A single machine infinite bus system

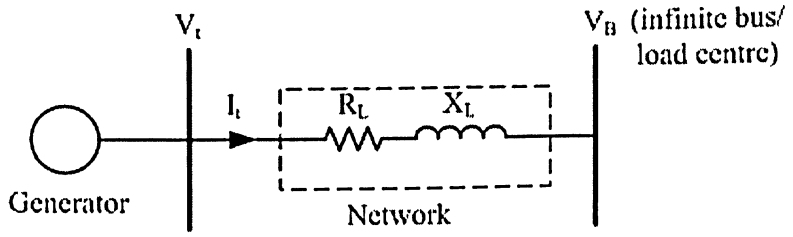

Figure 2.6b: Connection of a generator to an equivalent power system network

In order to determine parameters for the network equivalent circuit, the generator is connected to the power system network under predefined power system operating conditions. In practice, the typical predefined conditions are specified as the generator terminal voltage V_t and the supplied power P_t. Hence, the terminal generator current I_t can be determined.

2.5 Generator magnetic saturation

In order to have a better evaluation for the performance of the generator excitation control, it is important to take the magnetic saturation effects into consideration.

Since the leakage flux paths are mostly in the air-gap, the generator saturation equations can be written, with an assumption that the leakage inductances and the iron saturation are independent from each other, as below

$$\begin{aligned} L_{ads} &= K_{sd} L_{adu} \\ L_{aqs} &= K_{sq} L_{aqu} \end{aligned} \tag{2.20}$$

where,

L_{adu}, L_{aqu}: the unsaturated values of the mutual inductances L_{ad} and L_{aq}

K_{sd}, K_{sq}: the saturation factors

Figure 2.7 shows a representation of generator saturation characteristic. In the figure, the increment or change of flux linkage ψ_I represents the difference between the calculated air-gap flux linkage ψ_{T2} and the actual saturated air-gap flux linkage ψ_a. The difference in the air-gap flux linkage is an exponential function as follows,

$$\psi_I = A_{SAT} e^{B_{SAT}(\psi_a - \psi_{T1})} \tag{2.21}$$

In (2.21), ψ_{T1} stands for the threshold value of saturation. The constants A_{SAT} and B_{SAT} can be obtained from the generator's manufacture specifications.

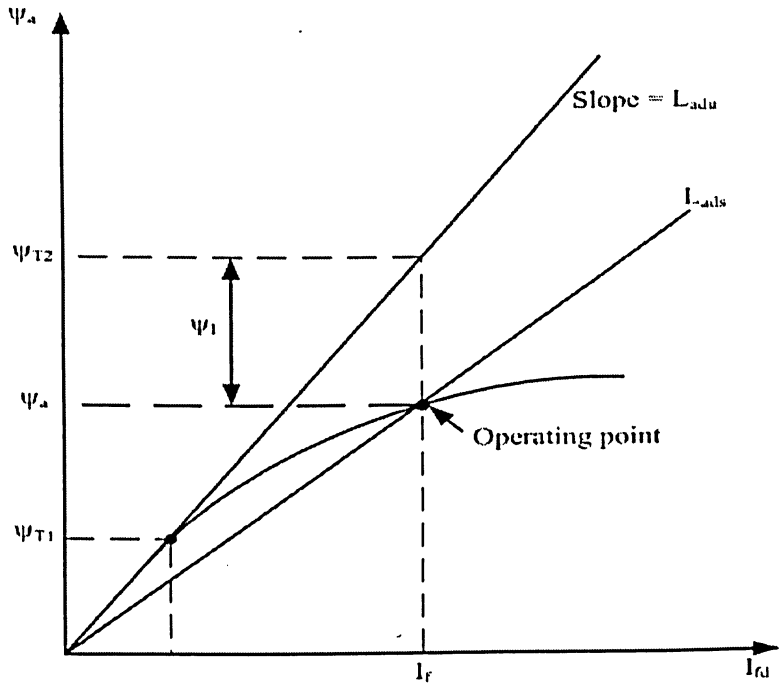

Figure 2.7: Representation of saturation characteristic

The saturation factor K_{sd} can be determined from the air-gap flux as in the following steps:

$$\psi_a = \sqrt{\psi_{ad}^2 + \psi_{aq}^2} \tag{2.22}$$

$$K_{sd} = \frac{\psi_a}{\psi_a + \psi_l} \tag{2.23}$$

The q-axis saturation factor K_{sq} is generally assumed to be 1 per-unit for a salient pole generator, because there is no significant variation with L_{aq} due to its flux mostly occurring in the air-gap.

2.6 Generator magnetic saturation

A simplified generator excitation system model is shown in Figure 2.8. The exciter is defined as a dc source that supplies power to the generator field winding.

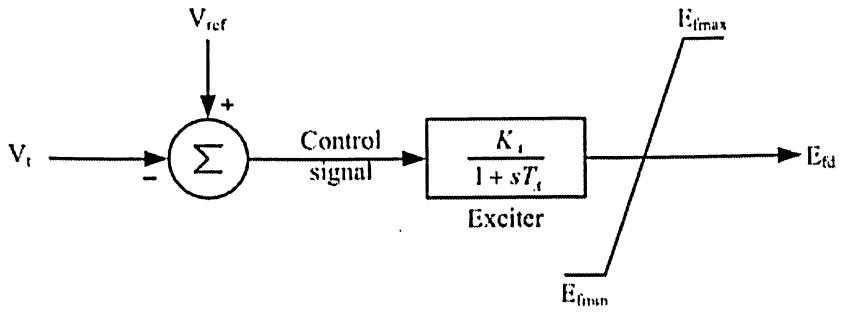

Figure 2.8: Excitation system block diagram

This excitation system is mathematically represented by the first order model as below,

$$\frac{dE_{fd}}{dt} = \frac{1}{T_A}\left[K_A(V_{ref} - V_t) - E_{fd}\right] \tag{2.24}$$

$$E_{f\min} \le E_{fd} \le E_{f\max}$$

where,

K_A, T_A: the AVR gain and its time delay constants respectively

V_{ref}: the reference voltage

V_t: the terminal voltage

2.7 Generator power system stabilizer model

The power system stabilizer is used in the excitation systems of a synchronous machine for the purpose of enhancing the dynamic stability of power generating systems. A power system stabilizer using speed, power or frequency as an input signal when applied with a high initial response excitation system is effective in damping low-frequency machine rotor oscillation. In order to provide damping of the oscillations of the synchronous machine's rotor, the PSS produces a component of torque in phase with rotor speed deviations.

The mentioned PSS structure is considered to be fixed and is tuned considering a set of nominal operating conditions and system parameters. However, such a fixed structure optimum PSS would provide sub-optimum performance under variations in system parameters and operating conditions. The power system can also be unstable due to negative damping effects of the PSS on the rotor.

In this project, the IEEE type ST1 AVR and PSS excitation system shown in Figure 2.9 is considered for the study and evaluation.

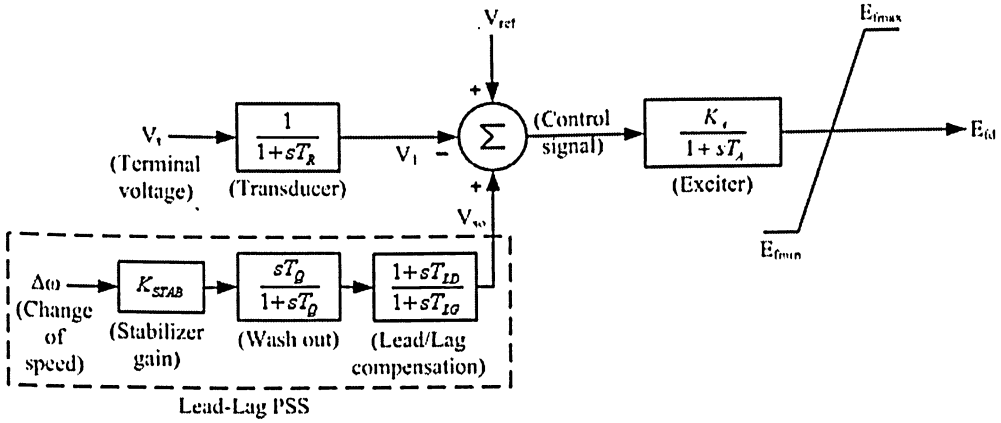

Figure 2.9: System block diagram of AVR and PSS excitation system

As illustrated in the block diagram, a conventional lead-lag PSS is installed in the feedback loop to generate a stabilizing signal V_{SO}. This PSS controller structure consists of a stabilizer gain K_{STAB}, a washout block and a phase compensation block.

The output signal of PSS is a voltage signal, as noted V_{SO}, and added as an input signal to the AVR/exciter. For the PSS structure shown in Figure 2.9, the equation can be given by

$$V_{SO} = K_{STAB}\left(\frac{sT_Q}{1+sT_Q}\right)\left(\frac{1+sT_{LD}}{1+sT_{LG}}\right)\Delta\omega \qquad (2.25)$$

where, T_Q is the washout circuit time, T_{LD} and T_{LG} are lead and lag time constants of PSS respectively.

In this particular controller structure, the washout block, $sT_Q / (1+sT_Q)$, is used to reduce the over-response of the damping during severe events. Alternatively, the washout block serves as a high-pass filter, with a time constant that allows the signal associated with oscillations in rotor speed to pass unchanged, but does not allow the steady state changes to modify the terminal voltages.

Since the PSS must produce a component of electrical torque in phase with the speed deviation, phase lead block circuits are used to compensate for the lag between the PSS output and the control action, the electrical torque. The number of lead-lag blocks needed depends on the particular system and the tuning of the PSS. In practice, two or more first order lead-lag blocks may be used to achieve the desired phase compensation.

The PSS gain K_{STAB} determines the amount of damping. This gain is an important factor as the damping provided by the PSS increases in proportion to an increase in the gain up to a certain critical gain value, after which the damping begins to decrease.

All of the variables of the PSS must be determined for each type of generator separately because of the dependence on the machine parameters. The power system dynamics also influence the PSS values.

Chapter 3

TEST SYSTEM

3.1 Generator and power system parameters

Figure 3.1 shows a machine infinite bus system configuration for the evaluation of power system stability in this project. In this diagram, the reactance of the transformer is labeled as X_T. The reactance of two transmission lines are X_{L1} and X_{L2} respectively.

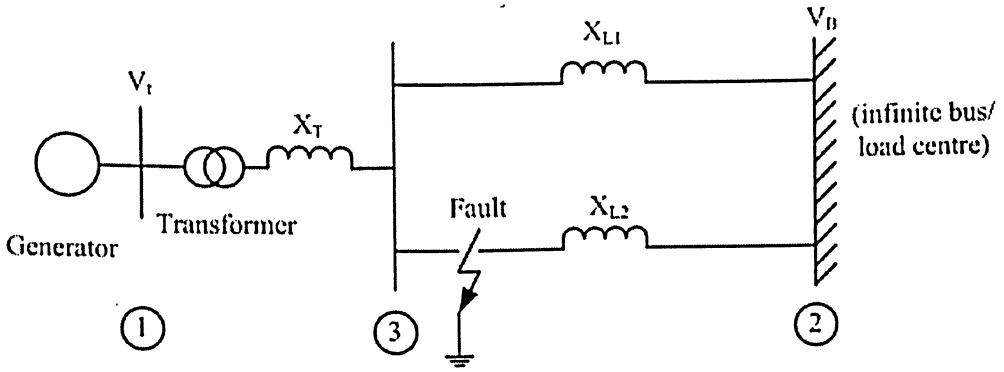

Figure 3.1: A generator to power system network model

The generator nameplate, the transformer and line impedances for the system are given in Table 1. The system saturation factors and the excitation control system parameters are listed in Table 2 and 3 respectively. All per-unit parameters are on a 555 MVA, 24 KV base.

Generator	Parameters	
S = 555 MVA	$X_d = 1.81$	$R_a = 0.003$
V = 24 KV	$X_q = 1.76$	$R_{fd} = 0.0006$
f = 60 Hz	$X_l = 0.16$	$R_{1d} = 0.0284$
Number of poles =2	$X_{fl} = 0.165$	$R_{2q} = 0.0237$
H = 3.5 MWs/MVA	$X_{1d} = 1713$	$R_{1q} = 0.0062$
$K_D = 0$	$X_{1q} = 0.7252$	$X_T = 0.15$
	$X_{2q} = 0.125$	$X_{L1} = 0.5$ $X_{L2} = 0.95$

Table 1: Generator nameplate and parameters

Saturation values
$A_{SAT} = 0.031$
$B_{SAT} = 0.031$
$\psi_{T1} = 0.8$
$\psi_{T2} = \infty$

Table 2: System saturation factors

AVR and PSS parameters	
AVR	PSS
$K_A = 200$	$K_{STAB} = 9.5$
$T_R = 0.015s$	$T_Q = 1.41\ s$
$E_{fmax} = 7.0$	$T_{LD} = 0.154\ s$
$E_{f\min} = 6.4$	$T_{LG} = 0.033\ s$

Table 3: AVR and PSS excitation control parameters

3.2 Derivation of generator equations

Generator quantities

Phasor representation:

For a synchronous generator under balanced, steady-state operation, the stator phase voltages in *dq0* reference frame can be written as

$$\begin{cases} e_d = E_m \cos(\theta - \omega t - \alpha) \\ e_q = E_m \sin(\theta - \omega t - \alpha) \end{cases} \tag{3.1}$$

The angle θ by which the d-axis leads the axis of phase a is given by

$$\theta = \omega_r t + \theta_0$$

where θ_0 is the value of θ at t=0. Assume that θ_0 =0, then Equation (3.1) can be rewritten as

$$\begin{cases} e_d = E_m \cos\alpha \\ e_q = E_m \sin\alpha \end{cases} \tag{3.2}$$

From Equation (3.2), the phasor representation of the generator under a balanced steady-state operation is illustrated in the Figure 3.2.

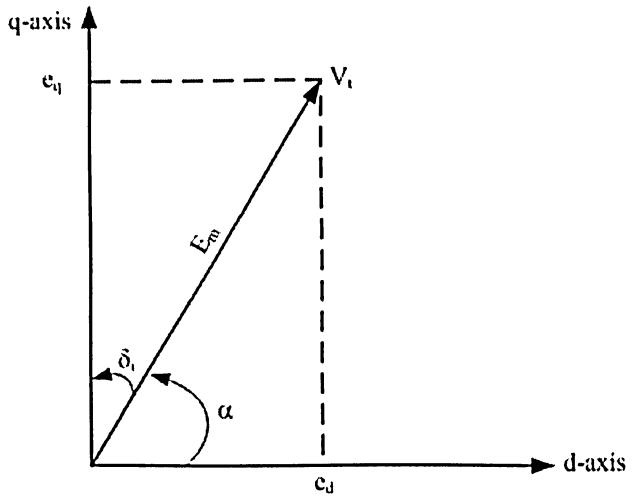

Figure 3.2: Voltage components

From the phasor diagram, the generator terminal voltage:

$$V_t = e_d - je_q \tag{3.3}$$

where,

$$\begin{cases} e_d = V_t sin\delta_i \\ e_q = V_t cos\delta_i \end{cases} \tag{3.4}$$

If the power factor angle is ϕ, then

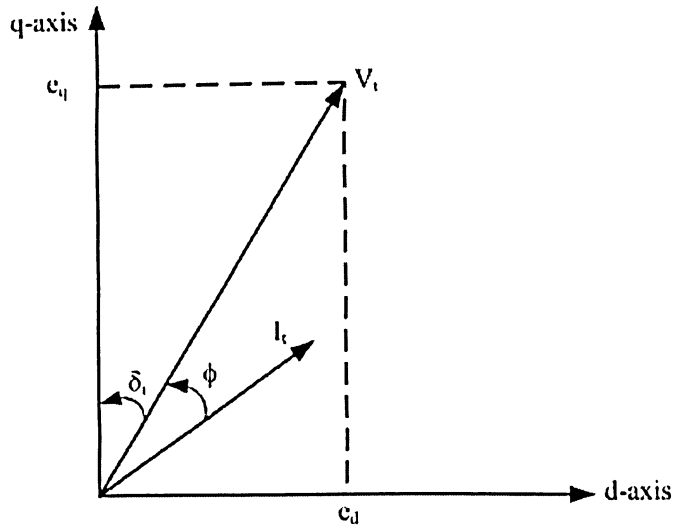

Figure 3.3: Current components

$$\begin{cases} i_d = I_t sin(\delta_i + \phi) \\ i_q = I_t cos(\delta_i + \phi) \end{cases} \tag{3.5}$$

The generator terminal current is

$$I_t = i_d + ji_q \tag{3.6}$$

The relationship between dq components of armature terminal voltage and current are defined by Equation (2.18). Hence,

$$e_d = -\psi_q - R_a i_d = X_q i_q - R_a i_d \tag{3.7}$$

$$e_q = -\psi_d - R_a i_d = -X_d i_d + X_{ad} I_{fd} - R_a i_q \tag{3.8}$$

If the voltage E_q is defined as:

$$
\begin{aligned}
E_q &= E_t + I_t(R_a + jX_q) \\
&= (e_d + je_q) + (i_d + ji_q)(R_a + jX_q) \\
&= j(I_{fd}X_{ad}) - ji_d(X_d - X_q)
\end{aligned}
\tag{3.9}
$$

The corresponding phasor diagram for E_q is shown in Figure 3.4. Note that the angle δ_i is referred to as the internal rotor.

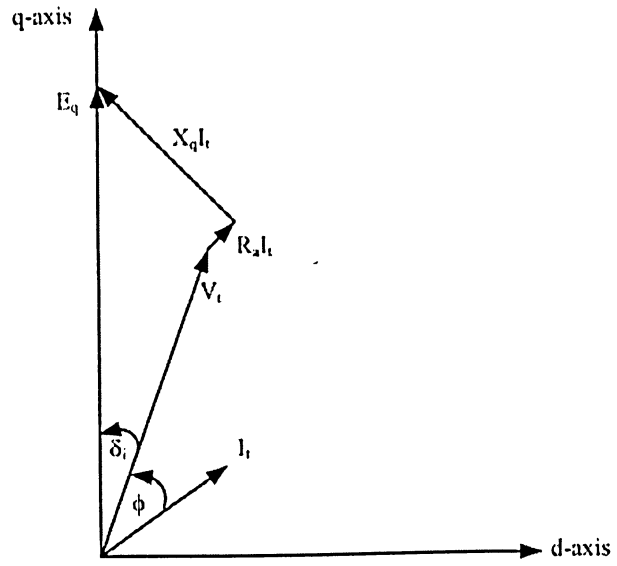

Figure 3.4: Phasor diagram of E_q in dq frame

Real and Reactive power:

$$
\begin{aligned}
S &= E_t I_t^* \\
&= (e_d + je_q)(i_d - ji_q) \\
&= P_t + jQ_t
\end{aligned}
$$

Hence,

$$
P_t = e_d i_d + e_q i_q \tag{3.10}
$$

$$Q_t = e_q i_d - e_d i_q \tag{3.11}$$

The steady-state torque is also given by:

$$\begin{aligned} T_e &= \psi_d i_q - \psi_q i_d \\ &= (e_d i_d + e_q i_q) + R_a (i_d^2 + i_q^2) \\ &= P_t + R_a I_t^2 \end{aligned} \tag{3.12}$$

Computing the steady-state values:

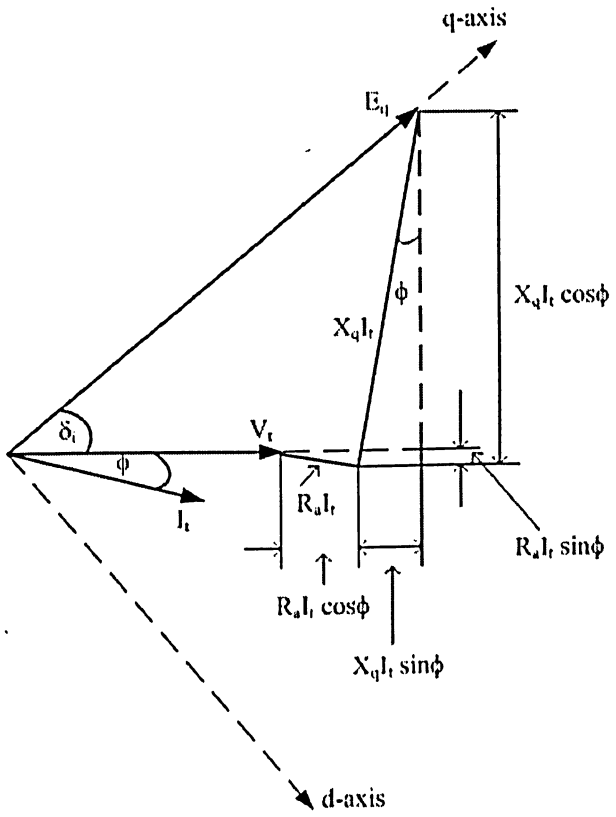

Figure 3.5: Steady state phasor diagram

From the given terminal active power P_t, reactive power Q_t, and generator terminal voltage V_t, the corresponding terminal current I_t and power factor ϕ are calculated as follows,

$$I_t = \frac{\sqrt{P_t^2 + Q_t^2}}{V_t}$$
$$\psi = cos^{-1}(P_t / V_t I_t)$$

The internal rotor angle δ_i can be determined as below,

$$\delta_i = tan^{-1} \frac{X_q I_t cos\phi - R_a I_t sin\phi}{V_t + R_a I_t cos\phi + X_q I_t sin\phi}$$

The dq components of stator voltage and current are given by

$$e_d = V_t sin\delta_i$$
$$e_q = V_t cos\delta_i$$
$$i_d = I_t sin(\delta_i + \phi)$$
$$i_q = I_t cos(\delta_i + \phi)$$

The remaining generator quantities:

$$i_{fd} = \frac{e_q + i_q R_a + X_d i_d}{X_{ad}}$$
$$e_{fd} = R_{fd} i_{fd}$$
$$\psi_{fd} = (L_{ad} + L_{fl}) i_{fd} - L_{ad} i_d$$
$$\psi_{1d} = L_{ad}(i_{fd} - i_d)$$
$$\psi_{1q} = \psi_{2q} = -L_{aq} i_q$$
$$\psi_d = e_q + R_a i_q$$
$$\psi_q = -e_d - R_a i_d$$

The torque can be computed as follows,

$$T_e = P_t + R_a I_t^2$$

The saturation effects:

The saturation air-gap flux is determined as follows:

$$\psi_a = \sqrt{\psi_{ad}^2 + \psi_{aq}^2}$$
$$\psi_{ad} = e_q + R_a i_q + i_d L_l$$
$$\psi_{aq} = -e_d - R_a i_d + i_q L_l$$

It is noted that the air-gap flux is equal to the air-gap voltage in per-unit, i.e., $\psi_a = V_a$, and the air-gap voltage can be expressed as,

$$V_a = V_t + I_t\ (R_a + jX_l)$$

The incremental air-gap flux:

$$\psi_l = A_{sat} e^{B_{sat}(\psi_a - \psi_{t1})}$$

The saturation factor:

$$K_{sd} = K_{sq} = \frac{\psi_l}{\psi_a + \psi_l}$$

The inductances L_{ad} and L_{aq} are re-written as follows,

$$L_{ad} = K_{sd} L_{adu}$$
$$L_{aq} = K_{sd} L_{aqu}$$

Once the inductances are determined, the values of I_{fd} and e_{fd} can also be recalculated in order to determine the corresponding exciter output voltage.

3.3 Computer simulation steps

The initial values of the differential equation (2.19) that included δ, $\Delta\omega_r$ and ψ_{fd} need to be determined for the computer simulation.

The power angle δ by which V_B lags the q-axis or E_q can be found from the phasor diagram in Figure 3.6, i.e. $\delta = \delta_i + \angle V_t V_B$.

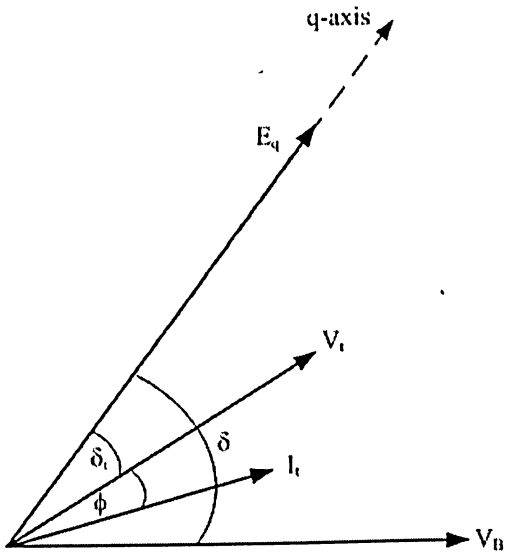

Figure 3.6: Phasor diagram of E_q, V_t, and V_B in dq frame

The generator is assumed to be operating at a steady-state condition before a disturbance is applied to test the response of the generator excitation control. Each state variable has a steady-state value. The all-time derivative $p\psi_{fd}$ is equal to zero. The flux-linkage can be calculated by using the equation:

$$\psi_{fd} = (L_{ad} + L_{fl})i_{fd} - L_{ad}i_d$$

and the electromagnetic torque:

$$T_e = P_t + R_a I_t^2$$

At the steady state, the generator runs at the rated speed, $\Delta\omega_r = 0$. All initial generator quantities can be determined.

For the transient process, the dq-axis currents are solved from the above network equations with updated state variables, which include ψ_{fd} and δ. As the flux linkage changes in the simulation process, the mutual inductance L_{ad} and L_{aq} are also recalculated to consider the effects of saturation.

In this report, the 4^{th}-order Runge-Kutta method is applied to obtain the solution for the differential equations. The following flowchart in Figure 3.7 illustrates the computer simulation process in each time-step.

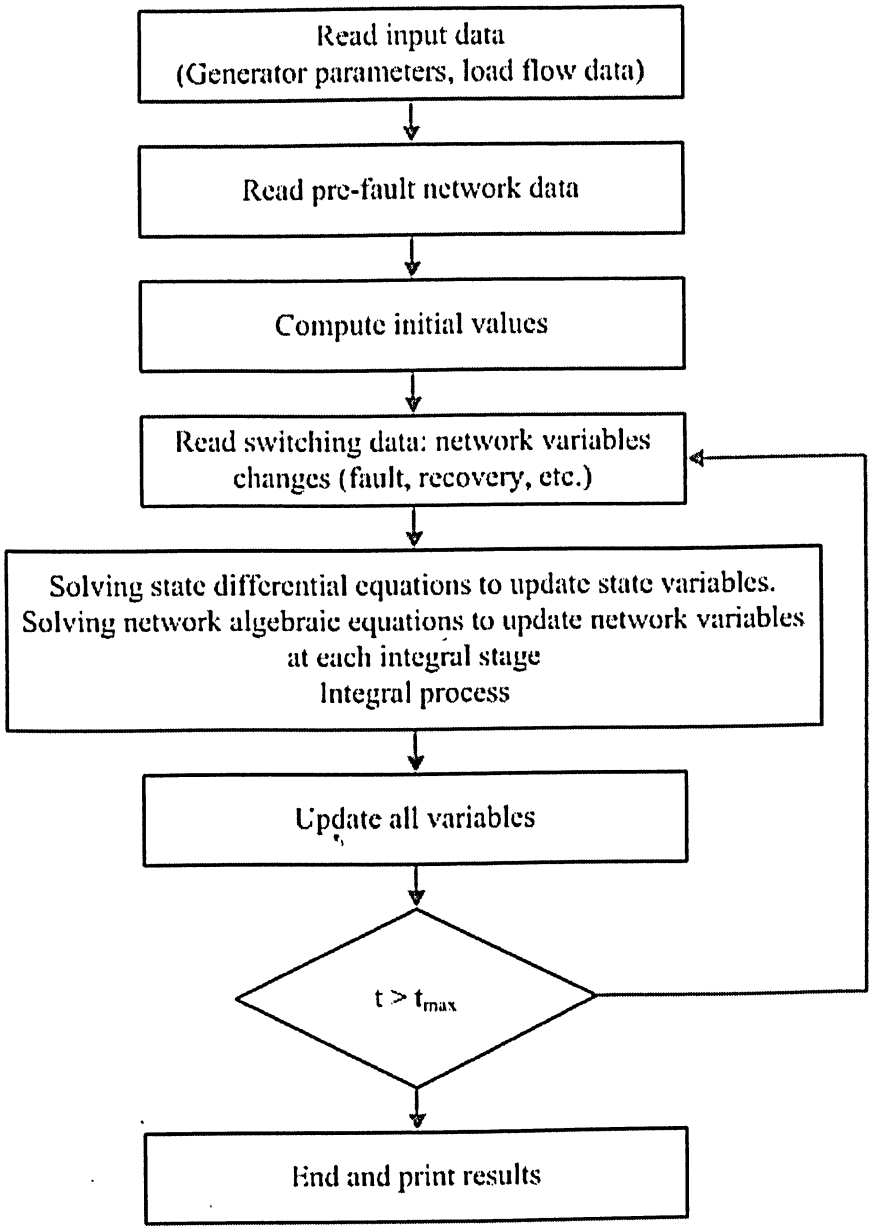

Figure 3.7: Flow chart diagram of the computer simulation process

Chapter 4

SIMULATION TEST SYSTEM

This chapter presents the computer simulation for the analysis of the generator excitation control developed in this project using Matlab/Simulink software package. A 3^{th} -order generator model is considered for software simulation and evaluation. The differential equations in (2.18) are employed for computations. The mechanical input torque is assumed to be a constant so that the generator excitation control can be evaluated.

4.1 Simulation test system

Figure 4.1 shows a typical single machine infinite bus system configuration for the evaluation of power system stability.

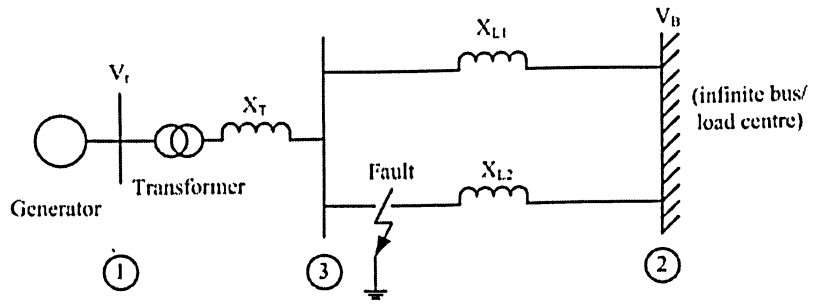

Figure 4.1: A generator to power system network model

In the above power network diagram, a single generator is connected to the transmission lines through an associated step-up transformer. Since the line equivalent resistance R_L is very small in comparison to the line reactance X_L, it

is often neglected in the power system study. The transformer has an impedance of X_T and its high voltage output terminal is connected to the two parallel transmission lines with impedances X_{L1} and X_{L2}. The system network delivers power to an infinite bus V_B. The parameters for the system are given in Chapter 3.

The design of the excitation control is subjected to the operating conditions of the generator. These conditions, also called the initial values, are to provide the per unit active power and terminal voltage as listed in Table 4.

Operating conditions
$P_T = 0.9$
$Q_T = 0.436$
$V_T = 1$

Table 4: Generator operating conditions

With the given above power system initial operating conditions, the pre-fault currents and power angles are determined and tabulated in Table 5.

Pre-fault values
$i_{d0} = 0.906$
$i_{q0} = 0.424$
$\delta_0 = 67.43^\circ$
$X_L = 0.473$

Table 5: Pre-fault currents, power angle, and total reactance of the power system network

4.2 Power system disturbance and alternative excitation controls

In this section, the large disturbance that is used for the case studies of the generator excitation control is caused by a three-phase fault on the generator bus. This disturbance assumes a three-phase fault occurring on the high voltage side of the generator transformer, at the point F shown in Figure 4.1. This fault lasts for 0.07 second. The fault is then cleared by the circuit breaker, and the faulted transmission line is removed from the power system network. This typical disturbance is used in the project to evaluate the stability of the power system.

The three alternative excitation controls are considered for case studies as follows:

- Manual control (i.e., constant E_{fd})
- AVR (i.e., static excitation system with only terminal voltage feedback)
- AVR + PSS (i.e., static exciter and speed deviance stabilizer $\Delta\omega$)

Case study 1: Manual excitation control system with disturbance caused by a three-phase on generator bus and its effects on the generator rotor angle δ, total power P_T, terminal voltage V_T, and field voltage E_{fd}

The results of the Matlab/Simulink simulation for the manual excitation control of a disturbance caused by a three-phase fault occurring on the generator bus as illustrated in Figure 4.1 are shown in Figure 4.2.

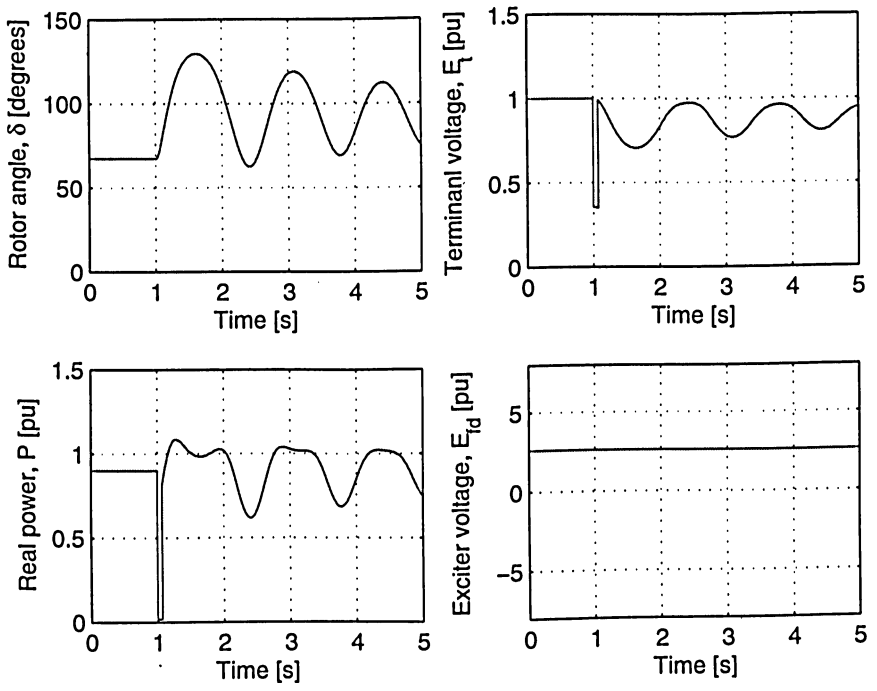

Figure 4-2: Fault effect with Manual excitation control

Figure 4.2 shows the simulation plot of the rotor angle δ. The pre-fault value of rotor angle is $67.4°$. As the fault happens, the rotor oscillation is large because of a low damping. The rotor angle is very slow to recover and this is not desirable in practice.

Similarly to what happens to the rotor angle, there is a large oscillation that associates with the network power after the fault happens. The overall power delivered to the network will transiently become stable.

Case study 2: AVR excitation control system with disturbance caused by a three-phase on generator bus and its effects on the generator rotor angle δ, total power P_T, terminal voltage V_T, and field voltage E_{fd}.

The results of the Matlab/Simulink simulation for the AVR excitation control of a disturbance caused by a three-phase fault occurring on the generator bus are shown in Figure 4.3.

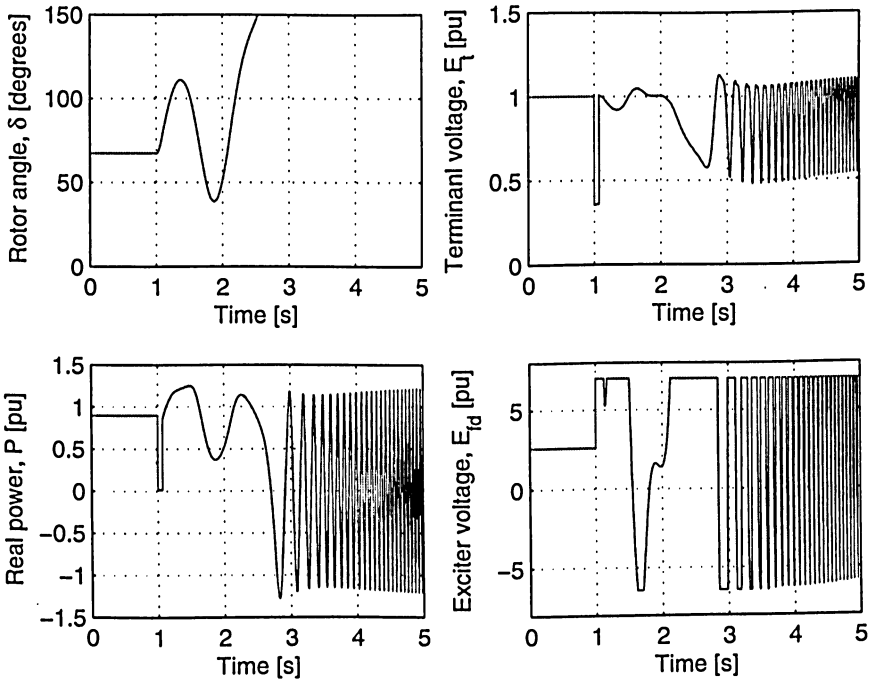

Figure 4.3: Fault effect with AVR excitation control

In the simulation plot of the rotor angle δ, it can be observed that the first oscillation rotor angle swing is smaller than that of the manual E_{fd} excitation control. The reason is that the AVR has a higher voltage gain to speed up the system response in overall. However, the rotor angle becomes to lose its synchronism in the subsequent swing due to the negative damping effect. The total network power, generator terminal voltage and output exciter voltage are unstable and oscillated as the result.

Case study 3: AVR and PSS excitation control system with disturbance caused by a three-phase on generator bus and its effects on the generator rotor angle δ, total power P_T, terminal voltage V_T, and field voltage E_{fd}.

In order to overcome of the negative damping drawback with the use of AVR alone, the PSS control is needed to enhance the stability of power system network. The action to PSS is as a phase-lead network to increase the phase margin, and hence, providing supplemental damping to the oscillation of the synchronous generator rotor.

The results of the simulation for the AVR + PSS excitation control are shown in Figure 4.4. From the simulation plot, it can be observed that the generator rotor angle is transiently stable after its third swing. Hence, the total power, generator terminal voltage, exciter output voltage are quickly to recover after the disturbance happens in the system.

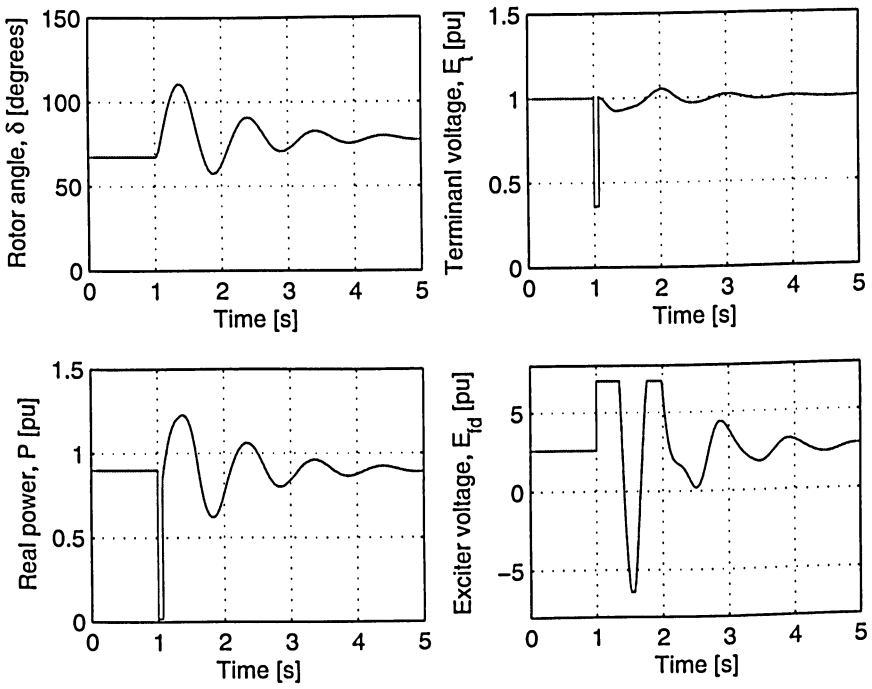

Figure 4.4: Fault effect with AVR and PSS excitation control

4.3 Comparisons of the three excitation control methods

Figure 4.5 shows the comparisons of the three excitation methods. The AVR and PSS excitation control scheme has been clearly shown to be more effective than the other two stand alone, namely the Manual and AVR control schemes.

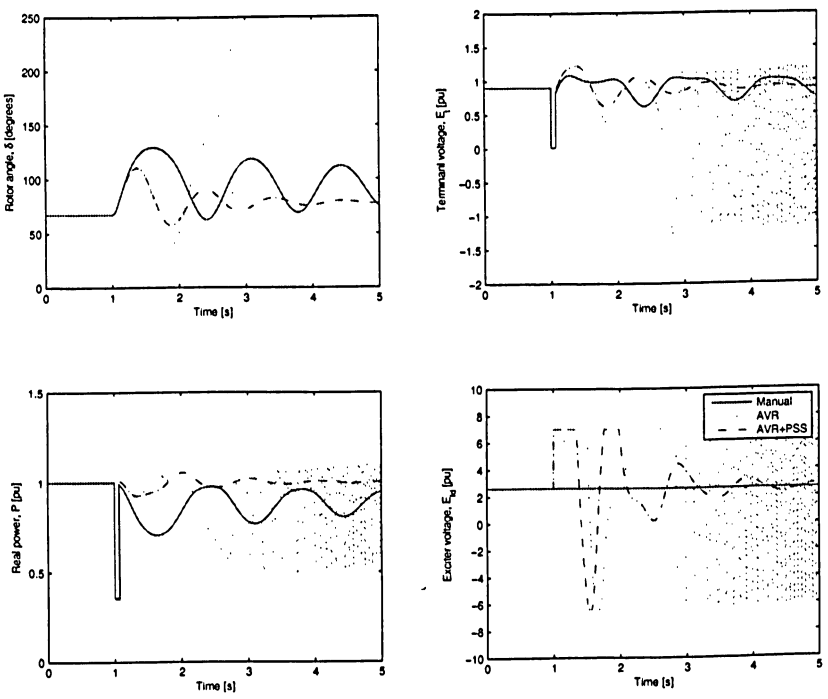

Figure 4.5: Comparison of the three excitation control methods

Chapter 5

CONCLUSION

This project has successfully completed the study and the design verification of an optimal excitation control system, named the Power System Stabilizer, for the utility generator.

The effectiveness of the AVR and PSS excitation control scheme is investigated through Matlab/Simulink computer simulations. It is shown that the use of AVR and PSS has achieved the best response for the power system stability comparing to the manual or AVR excitation control method.

The PSS is not a robust model for the excitation control, comparing to current available technologies that develop to enhance the power system stability, due to its parameters are tuned around a steady-state operating point. However, the design of the combination AVR and PSS excitation control scheme has some features as follows:

- Simplicity of the design that allows the implementation of the power system generator excitation control in real-time.
- The required input control signal for the PSS, the rotor speed $\Delta\omega$, are practically measurable from the circuit.

5.1 Major Tasks Accomplished

The major tasks accomplished in the project are:

- The project investigated the cause of power system oscillation, the need for generator excitation control, and the conventional automatic voltage regulator with the addition of the power system stabilizer.

- The modeling of the synchronous generator, power system network, excitation system for the design of power system optimal excitation control are provided in the project.

- A computer simulation software program using Matlab/Simulink was designed and can be used by other researchers for the power system stability study.

- Study cases are presented to study the effectiveness of the PSS excitation control scheme.

5.2 Future work

The following lists recommended work in future study for power system stability.

- Investigation on other excitation control methods such as the popular model predictive control technology, fuzzy-logic and artificial neural networks.

- Researching an effective real-time control of the power system generator excitation.

- Implementation of the PSS on the multi-machine system.

APPENDIX

Matlab/Simulink model

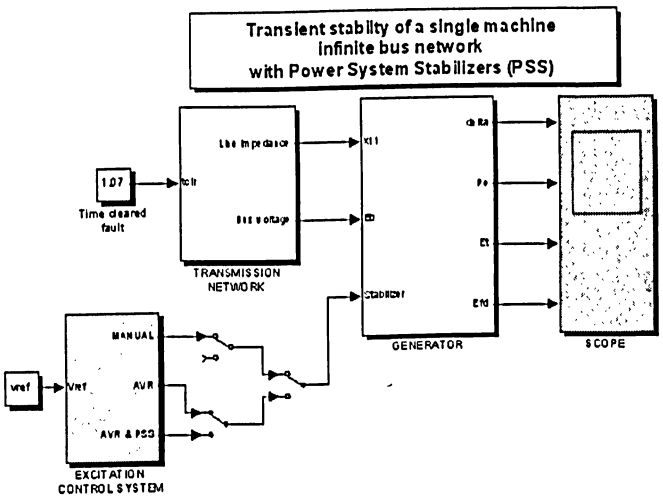

Figure A.1: A generator to power system network model

Transmission line network

```
function [X11,eb]  = fcn(eb0,tclr,t)

if t<1 X11=0.4752; eb=eb0;
   elseif t>=1 & t<tclr X11=0.15; eb=0;
   else X11=0.65; R11=0; eb=eb0;
end
```

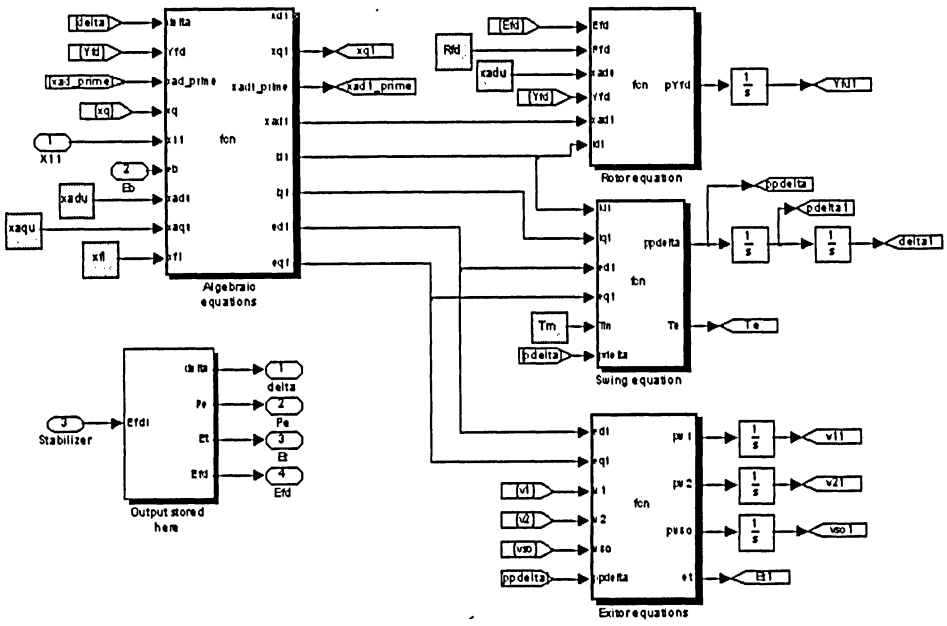

Figure A.2: Simulink model of a synchronous generator

Algebraic equations:

```
function [xd1,xq1,xad1_prime,xad1,id1,iq1,ed1,eq1] =
fcn(delta,Yfd,xad_prime,xq,x11,eb,xl,xadu,xaqu,xfl,Ra,Yt1,Asat,Bsat)
img = 1i;
ebd=eb*sin(delta); ebq=eb*cos(delta); g=ebd; h=(Yfd/xfl)*xad_prime-ebq;
l=Ra; m=x11+xq;
n=x11+xad_prime+xl;
id1=(m*h-l*g)/(l*l+m*n); iq1=(l*h+n*g)/(l*l+m*n);
ed1=ebd-x11*iq1; eq1=ebq+x11*id1;

% consider saturation
Ea=(ed1+img*eq1)+(id1+img*iq1)*(Ra+img*xl);ea=abs(Ea);
   if ea<Yt1 Ksat=1;
   else Ksat=ea/(ea+Asat*exp(Bsat*(ea-Yt1)));
end
xad1=xadu*Ksat; xaq1=xaqu*Ksat; xd1=xad1+xl; xq1=xaq1+xl;
xad1_prime=xad1*xfl/(xad1+xfl);
```

Rotor equations:

```
function pYfd    = fcn(Efd,Rfd,xadu,wo,Yfd,xad1,id1,xl)
% Rotor equation
%       p(Yfd)=wo(efd-Rfd*ifd)
% where efd=Efd*Rfd/xadu;ifd=(Yfd+xad*id)/(xad+xl)
efd=Efd*Rfd/xadu; ifd=(Yfd+xad1*id1)/(xad1+xl); pYfd=wo*(efd-Rfd*ifd);
```

Swing equations:

```
function [ppdelta,Te]   = fcn(id1,iq1,ed1,eq1,Ra,wo,H,Tm,pdelta)

% swing equations
%       p(pdelta)=wo/H/2*(Tm-Te-KD(pdelta))          (2)
% where Tm=0.903;KD=0

KD=0;   Te=id1*ed1+iq1*eq1+Ra*(id1*id1+iq1*iq1);   ppdelta=wo/H/2*(Tm-
Te-KD*(pdelta));
```

Exciter equations:

```
function [pv1,pv2,pvso,et]     = fcn(ed1,eq1,v1,v2,wo,vso,ppdelta)

% AVR equation:
% p(v1)=(et-v1)/TR
TR=0.015; et=sqrt(ed1*ed1+eq1*eq1); pv1=(et-v1)/TR;

% PSS equations:
% p(v2)=Kstab/wo*(p(pdelta))-v2/TQ
TQ=1.41; Kstab=9.6; pv2=Kstab/wo*(ppdelta)-v2/TQ;

% p(vso)=(TLD*p(v2)+v2-vso)/TLG
TLD=0.154; TLG=0.033; pvso=(TLD*pv2+v2-vso)/TLG;
```

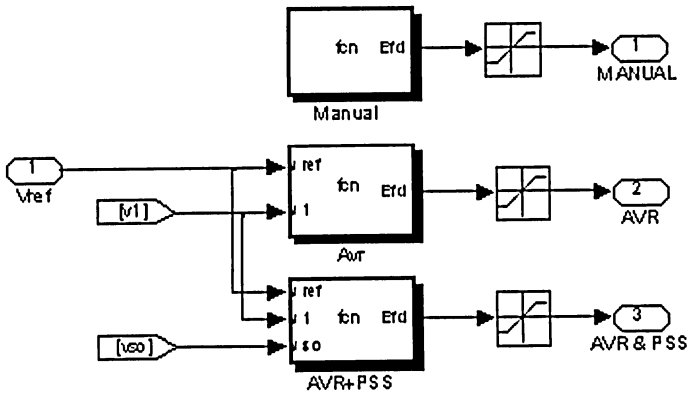

Figure A.3: Simulink model of the power system stabilizer

Manual control:

```
function Efd = fcn(Efd0)
Efd=Efd0;
```

AVR:

```
function Efd = fcn(vref,v1,KA)
Efd=KA*(vref-v1);
```

AVR+PSS:

```
function Efd = fcn(vref,v1,vso,KA)
Efd=KA*(vref-v1+vso);
```

BIBLIOGRAPHY

[1] P. Kundur. *Power System Stability and Control.* McGraw-Hill Publishing Company, 1994, pp699-954.

[2] P. M. Anderson, A.A. Fouad. *Power System Control and Stability.* IEEE Press, John Wiley & Sons, Inc., Publication, 2003.

[3] IEEE Digital excitation Application Taskforce, *"Digital Excitation Technology – A review of features, functions, and benefits"*, IEEE Transactions on Energy Conversion, Vol.12, No.3, September 1997.

[4] M. A. Cybenko, Y. L. Abdel-Magid. *"Analysis of Power System Stability Enhancement and Facts-Based Stabilizers, pp 2-8", Technical Report.* Department of Electrical Engineering, King Fahd University, Dhahran, Saudi Arabia, 2004.

[5] Hadi Saadat. *Power System Analysis.* McGraw-Hill Publishing Company, 1999.

[6] G. Rogers. *Power System Oscillations.* Kluwer Academic Publishers, 2000, pp28-50.

[7] Y. N. Yu. *Electrical Power System Dynamics.* Academic Press, 1983, pp95-137.

[8] J. Qingxiang. *"Synchronous Generator Excitation Control Based on Model Predictive Control", Thesis Report.* Department of Electrical & Computer Engineering, Ryerson University, Toronto, Canada, 2005.

[9] IEEE Std 1110-2002. *"IEEE Guide for Synchronous Generator Modeling Practices and Applications in Power System Stability Analyses, pp 6-28", Technical Report.* IEEE Power Engineering Society, New York, USA, 2003.

[10] IEEE Std 1159-1995. *"IEEE Recommended Practice for Monitoring Electric Power Quality, pp 1-9", Technical Report.* IEEE Power Engineering Society, 2005.

[11] S. Gilbert, H. Le-Huy. *"Digital Simulation of Power Systems and Power Electronics using the Matlab/Simulink Power System Blockset", Technical Report.* IEEE Power Engineering Society, 2000.

[12] R. Sadikovic. *" Single Machine Infinite Bus System", Internal Report.* Zurich, 2003.